COMPARISON OF DIFFERENT REAR CONTACTING APPROACHES FOR INDUSTRIAL PERC SOLAR CELLS ON MC-SI WAFER

L. Gautero[1,2], D. Kania[1], J. Seiffe[1], A. Knorz[1], J. Specht[1],J. Nekarda[1], M. Hofmann[1], J. Rentsch[1], J.M. Sallese[2],   and R. Preu[1].

[1]Fraunhofer Institute for Solar Energy Systems, Heidenhofstrasse 2, D-79110 Freiburg im Breisgau, Germany
[2]Ecole Polytechnique Fédérale de Lausanne, 1015 Lausanne – Switzerland

ABSTRACT: The technology transfer of highly efficient solar cell concepts (i.e. passivated emitter and rear cell PERC) to industry can help reduce their production cost. This work appraises three different industrial approaches for the technology transfer and a conventional processing with a fair comparison. A significant improvement compared to conventional processing was obtained. All advanced approaches lead to an increase in open circuit voltage and short circuit current. This testifies to the benefits of improved passivation of the rear surface and a bettered light trapping. The optimal processing window for the advanced approaches has lower fill factor than the conventional processing. However, the reduction does not result in lower conversion potential. Finally, the PERC type devices deliver a significant increase of more than 0.4 % absolute in conversion efficiency. The structure which proved best was based on laser fired contacts (LFC). A maximum efficiency of 17.0 % has been achieved on 1.8 Ωcm multi-crystalline silicon.
Keywords: PERC, inkjet, laser ablation, multi-crystalline silicon.

1. INTRODUCTION

In recent published studies [1], a roadmap towards lower production cost was delineated. It features higher production volumes, higher efficiency silicon solar cells with respect to conventional present technology and lower silicon wafer thickness. This work addresses the two latter challenges by proposing optimized process sequences. Furthermore, these sequences are applied to multi-crystalline silicon (mc-Si), which has a lower intrinsic production cost.

The increased ratio of surface to volume draws the attention to surface passivation. The work will detail different options to locally contact the base through the passivation on the back surface.

The adaption of conventional screen printing techniques highlights the value of the here investigated technology transfers for the industry.

Different local contacting techniques were already presented in [2-4]. However, differences, especially in back surface passivation and starting material, hindered their direct comparison. This work aims to test each technique with equal starting conditions.

2. EXPERIMENT

The conventional processing is compared to advanced techniques able to structure the back surface.

2.1. Common process description

A large set of mc-Si wafers (p-type mc-Si, $\rho = 1.8\pm0.3$ Ωcm, full square, 156 mm side, 170 μm starting thickness) was processed following the description illustrated in Figure 1.

The standard quality material employed does not follow neighbouring criteria. However, to ensure a fair comparison between the processing variations in this work, a quality driven distribution amongst groups was performed. The details are given below.

An acetic texturing step was performed on an industrial line to set up all "as cut" wafers. After shipping to the PVTEC laboratory [5], they were further processed with a single side etching [6] on the rear side. These steps prepared a lowly reflecting front surface and a smooth back surface. This asymmetrical structure is advantageous for the light trapping [7] and for an enhanced passivation potential [8].

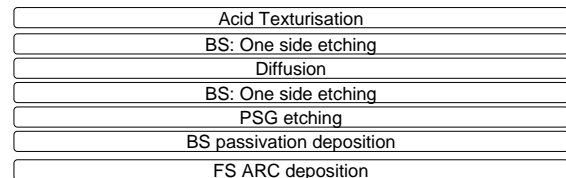| Acid Texturisation |
| :---: |
| BS: One side etching |
| Diffusion |
| BS: One side etching |
| PSG etching |
| BS passivation deposition |
| FS ARC deposition |

Figure 1 Common processing trunk. The cells, originally taken as cut from the ingot, are transformed in un-metallised solar cells.

The process continued with the creation of an n-type phosphorous emitter. To allow the deposition of the passivation coating directly on the semiconductor base, the diffused emitter was removed on the back surface.

The wafer was then coated with passivation layers on both sides using an inline PECVD system (SiNA, Roth and Rau). For this study an amorphous aluminium oxide (AlO_x) layer has been deposited on the back surface [9]. This layer was then capped with an amorphous silicon nitride (SiN_x) layer. On the front side, an anti-reflecting coating based on SiN_x was deposited.

At the end of the common processing trunk, all wafers were investigated for their effective lifetime. The distribution of the results had a low spread ($\tau_{eff} = 25\pm3$ μs). However, this measure does not imply the final performance of the device. However, it testifies to the quality of material and passivation.

2.2. Samples re-distribution and variation of processing

The un-metallised solar devices were then divided into groups. Attention was given to distribute uniformly the slightly different wafer effective lifetime. The new groups shared the same average effective lifetime. This expedient guarantees a fair comparison amongst the groups.

Three different pastes were selected for the realisation of the devices: paste A and B were selected for their lack of dielectric etching agents (glass frits) and their good bulk conductivity in their sintered form. Paste C, on the other hand, is an optimal candidate for the geometrically unconstrained formation of an aluminium back surface field (Al-BSF).

In order to apply the conventional processing, the passivation on the back surface was removed by exploiting a complete inkjet masking of the front side

(see double lined box in Figure 2). The passivation coating and its removal are performed in addition to the conventional processing.
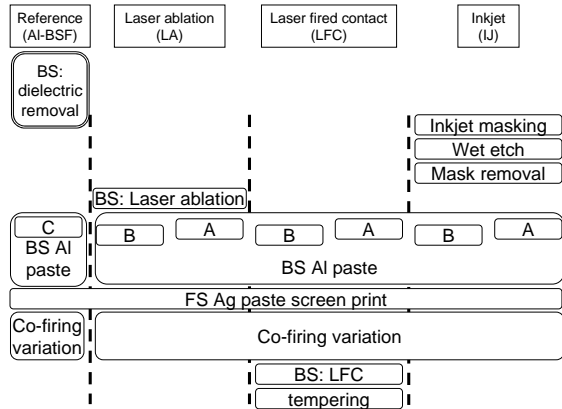

Figure 2 The devices realized from the process flow in Figure 1 were then processed with 4 different methods. These methods varied the approach to locally penetrate the otherwise isolating passivation. Furthermore, the paste was varied (A, B and C) along with the co-firing maximum set temperature.

One of the groups is distinguished by the formation of an Al-BSF on the rear surface. This is the current conventional processing method and is therefore used as a reference. The other three advanced processing methods, on the other hand, exploit the passivated back surface.

2.3. Laser ablation

The passivation layers can be ablated by means of laser ablation techniques (LA). Previous work on similarly deposited dielectric layers delivered the necessary experience to perform local opening [10]. The direct action of the laser pulse on the coating removes it entirely, leaving an undamaged silicon surface exposed. The subsequently screen printed metallic paste alloys on the local opening [11, 12], forming the contact. As for the other PERC cases below, the contacts have been distributed on the back as sketched in Figure 3.
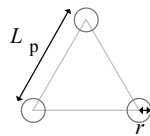

Figure 3 The contacts (small circles) are placed on the edges of adjacent equilateral triangles.

2.4. Laser fired contacts

In our labs, an alternative based on laser fired contacts (LFC) has been developed and improved repeatedly [13, 14]. The base is contacted after the sintering of the screen printed metals. A local heating by laser melts the aluminium, the dielectric layer, and a small quantity of silicon beneath. The re-crystallisation of this melt delivers the desired contact.

Subsequently, a tempering step cured the damage introduced by the process.

2.5. Inkjet masking

A selective masking by means of inkjet [15, 16] has been evaluated (IJ). The applied sequence covers the wafers entirely on the front with a wax mask. On the other hand, on the back surface a specifically designed wax mask left areas of the passivation dielectric exposed

(see Figure 3). The subsequent wet etch erodes the dielectric. Finally, the mask is removed in an acetone bath. The screen printed aluminium layer alloys during the sintering through the opening with the silicon beneath (as described for 2.3,)

Table 1 Details of desired metal coverage for each technique. A legend for the symbols is detailed in Figure 3.

Contact	Paste	Radius r (μm)	Pitch L_P (μm)
Al-BSF	C	∞	-
LA	A, B	25	450
LFC	A, B	30	500
IJ	A, B	47*	800

* This desired opening size was not matched. Instead, equivalent radiuses larger than 70 μm were observed after wet etching.

2.6. Metal coverage and passivation

The technologies chosen leave little room for the design of the contact radius. Each technique has its own range of allowed radiuses (see Table 1). To allow a fair comparison, a similar metal cover fraction has been performed for each group. Although this does not optimize the coverage for each technique, the calculated deviation from the maximum gain is less than 0.1% absolute (calculation performed with the tool developed internally [17]).

The dielectric coating employed on the back surface for this study is a stack of AlO_x and SiN_x. This stack has been tested in other parallel works for its passivation potential and its performance on solar cells. More details can be found elsewhere[9, 18].

3. RESULTS

3.1. Illuminated characterisation

The solar cells, after the processing (Figure 1 and Figure 2), are measured to investigate their behaviour at standard illumination conditions (AM1.5G). The well established characteristics are reported in Table 2 (open circuit voltage V_{OC}, short circuit current J_{SC}, conversion efficiency η, and fill factor FF).

Table 2 Average values for the optimal processing (in **bold**) and best solar cell values (in *italics*). The number of averaged cells is reported in brackets.

Contact	V_{OC} (mV)	J_{SC} (mA/cm^2)	η (%)	FF (%)
Al-BSF (5)	**613**	**33,5**	**15,8**	**76,8**
best	*614*	*33,5*	*16,1*	*78,2*
LA (7)	**625**	**34,9**	**16,4**	**75,4**
best	*626*	*34,9*	*16,9*	*77,4*
LFC (7)	**625**	**34,9**	**16,6**	**76,1**
best	*628*	*35,1*	*17*	*77,3*
IJ (5)	**618**	**34,5**	**16,2**	**76,2**
best	*624*	*34,8*	*16,8*	*77,5*

3.2. Internal quantum efficiency

For each structuring and each paste, solar cells were selected by the criteria of high short circuit current. These have been measured for their external quantum efficiency. By using the reflection of the metallised wafer it is possible to obtain the internal quantum efficiency. This in turn unveils the absorption efficiency of each cell structure (see Figure 4). The measurement was performed on the complete solar cell area under 0.1 suns bias light. Furthermore, from these curves it is possible to extract the effective diffusion length [19] (see Table 3).

Finally, the reflection of the back surface is empirically quantified as the reflection at long wavelength (also in Table 3).
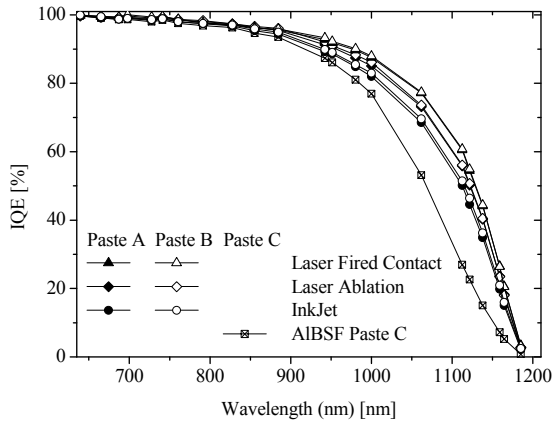

Figure 4 Measurements of the internal quantum efficiency for each cell structure. To underscore the difference of the back surface structure, only the long wavelengths are reported. Structures present almost overlapping curves even with different pastes

Table 3 Measured reflection at 1200 nm (R_{1200}) and calculated diffusion length (L_{Dn}) for the different structuring methods.

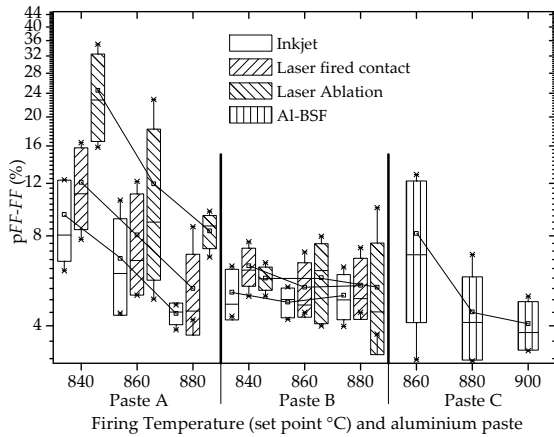| Structure	R_{1200} (%)			L_{Dn} (µm)		
Paste	A	B	C	A	B	C
Al-BSF	-	-	31	-	-	289
LA	52	50	-	436	487	-
LFC	55	54	-	513	551	-
IJ	48	48	-	348	373	-

3.3. Fill factors

Figure 5 Box-Whisker plot of the difference between the fill factor and the pseudo fill factor. This latter is obtained from a SunsVoc measurement. The squares indicate the average, the line in the box represents the median, box edges represent the standard deviation, and the whiskers indicate the 95% confidence interval. Note the logarithmic scale.

The difference of the pseudo fill factor p*FF* and the *FF*, as a consequence of their definition, is a direct and quantitative observation on the resistive path that the photogenerated current has to cover before reaching any external load. Before presenting this difference we detail that the absolute value of the p*FF* is homogeneous amongst all wafers (81±0.7).

The differences are plotted in Figure 5. Each group had 4 or more solar cells. The groups are divided by

aluminium paste, firing temperature, and the realised structure.

From the measurement of the finger bulk resistance performed on the front side grid, it can be inferred that the reference and the advanced processed samples shares the same front grid series resistance. This, in turn, supports a stronger relation between the plotted value (Figure 5) and the back surface structuring variations performed.

4. DISCUSSIONS

The trends and absolute values are used to discuss the performances of the implemented PERC structures.

The efficiency of all PERC type solar cells is significantly higher than the reference group Al-BSF (see Table 2). This can also be interpreted as a direct consequence of the increased diffusion length, which is distinctive for these groups (see Table 3). The experimental setting allows attributing the advantage to the better surface passivation of the back side.

Such results can be further enhanced by choosing a base material with a higher doping level. Indeed, mc-Si material is unaffected by boron-oxygen complexes. A low resistive base decreases the spreading resistance effect that affects PERC type solar cells with decreased *FF*. Simulations were conducted with the help of an analytical model [17]. By using the results of this work as input parameters, an increase up to 0.3 % abs. was calculated for a proper material choice on the best structure here presented (LFC).

4.1. Recombination at the back surface and increased photon collection

Due to the identical front side amongst the various groups, the variation of the open circuit voltage is directly traceable to the structure present on the back surface. A decrease in V_{OC} (less than 10 mV) is observed on back surface passivated samples between the lowest and the highest temperature. This can represent a wearing of the passivation layer. Details on the passivation layer behaviour are given elsewhere [18, 20]. However, its extent varies with the contacting scheme.

Except in their optimal process window, LA and IJ groups tend to limit the V_{OC} more than the LFC group by the same processing conditions. This observation infers a changing local passivation of the contact for LA and IJ.

Reflection measurements (see Table 3) reported the highest escape reflection (measured as the reflection of the finished solar cell at 1200 nm) for the LFC case. With this measurement a distinction on the light trapping of each structuring method is at hand. The difference can be attributed to undercutting phenomena of the aluminium paste at the local contacts during the firing [11]. These would increase further the metal fraction, reducing in turn the reflection of long wavelengths at the back surface and their eventual collection.

4.2. Back contacting comparison

A difference emerges amongst the PERC structures between the case of IJ and the two other groups. Inkjetted cells achieve on average a lower V_{OC} and lower J_{SC} result. This can be attributed to the metal coverage being larger than intended. However, the increased metal fraction of the inkjetted samples results in an increase of the *FF*. This is also confirmed by calculations [17].

A main difference between the LA group and the LFC group is the average *FF*. Although V_{OC} and J_{SC} are

similar, the different contact formations influence the local contact resistance. The LFC process has a contact resistance equal for all temperatures. Therefore, it depends on the firing conditions only through the changing lateral conductivity of the sintered paste. On the other hand, the LA (as well as IJ) additionally undergoes the influence of how the Al paste melts with silicon to form a contact [11].

4.3. Considerations on contact formation and lateral conductivity

In a parallel experiment [11, 12], it has been verified that the inkjet structure presents increased openings as well, due to an undercut phenomena. Furthermore, by indexing the quality of the contact by the thickness of the aluminium doped region found at the ohmic interface, it has been concluded that, apart from the processing parameters, the paste also contributes to better contacting.

From the paste comparison in Figure 5, assuming that the sintering of the front paste develops in the same way for all advanced structuring under equal firing conditions, we can say that paste A is limiting the *FF* with its lateral conductivity, which has not yet reached a necessary negligible value.

4.4. Edge removal

Unfortunately, after the emitter diffusion, the one side etching step modified the emitter on the edges of the front side. This was remarked after the metallisation sequence. The adopted solution was to reduce the side length of the wafers to 125mm.

5. CONCLUSION

The comparison remarks on different approaches for the industrial realisation of PERC concepts. All techniques attains significant improvements with respect to the conventional processing in their optimum processing configuration (p_{test}<5%). The increase is a 0.4 % abs. for inkjetted samples, a 0.6 % abs for laser ablated samples and a 0.8 % abs for laser fired contacts.

First insights on the influence of the rear side contact formation and its influence on the resistance path were also put to evidence. The process defects which lead to a lower performance for the inkjet samples underscore the importance of quality for these processes targeting high efficiency.

Conversion efficiencies as high as 17.0 % have been achieved on p-type mc-Si (ρ = 1.8±0.3 Ωcm, full square, down sized to 125 mm) with a starting thickness of 170 μm.

6. ACKNOWLEDGEMENTS

REFERENCES

1. del Canizo, C., G. del Coso, and W.C. Sinke, *Crystalline silicon solar module technology: towards the 1€ per watt-peak goal.* Progress in Photovoltaics: Research and Applications, 2009. **17**: p. 199-209.
2. Lauermann, T., et al. *Enabling dielectric rear side passivation for industrial mass production by developing lean printing-based solar cell processes.* in *Photovoltaic Specialists Conference (PVSC), 2010 35th IEEE.* 2010. Honolulu, HI.
3. Agostinelli, G., et al. *Local contact structures for industrial perc-type solar cells.* in *Proceedings of the 20th European Photovoltaic Solar Energy Conference.* 2005. Barcelona, Spain.
4. Hofmann, M., et al. *Firing stable surface passivation using all-PECVD stacks of SiO$_x$:H and SiN$_x$:H.* in *Proceedings of the 22nd European Photovoltaic Solar Energy Conference* 2007. Milan, Italy.
5. Biro, D., et al. *PV-Tec: retrospection to the three years of operation of a production oriented research platform.* in *Proceedings of the 24th European Photovoltaic Solar Energy Conference.* 2009. Hamburg, Germany.
6. Kästner, G., et al. *Single side polish etching for the rear side of crystalline silicon wafers.* in *This Conference, 25th EUPVSEC.* 2010. Valencia.
7. Kray, D., *Hocheffiziente Solarzellenstrukturen für kristallines Silicium-Material industrieller Qualität,* in *Fakultät für Physik.* 2004, Universität Konstanz: Konstanz. p. 152.
8. Rentsch, J., et al. *Single side etching - key technology for industrial high efficiency processing.* in *Proceedings of the 23rd European Photovoltaic Solar Energy Conference.* 2008. Valencia, Spain.
9. Saint-Cast, P., et al. *High efficiency p-type perc solar cells applying pecvd alox layers.* in *This Conference, 25th EUPVSEC.* 2010. Valencia.
10. Knorz, A., et al., *Selective laser ablation of SiN$_x$ layers on textured surfaces for low temperature front side metallizations.* Progress in Photovoltaics: Research and Applications, 2008. **2008**: p. 1-10.
11. Grasso, F.S., et al. *Characterisation of local Al BSF formation for industrial PERC solar cell structure.* in *This Conference, 25th EUPVSEC.* 2010. Valencia.
12. Grasso, F.S., et al. *Characterization of aluminium screen-printed local contacts.* in *2nd Workshop Metallization for Crystalline Silicon Solar Cells.* 2010. Constance, Germany.
13. Nekarda, J., et al. *LFC on screen printed aluminium rear side metallization.* in *Proceedings of the 24th European Photovoltaic Solar Energy Conference.* 2009. Hamburg, Germany.
14. Gautero, L., et al. *All-screen-printed 120-μm-thin large-area silicon solar cells applying dielectric rear passivation and laser-fired contacts reaching 18% efficiency.* in *Proceedings of the 34th IEEE Photovoltaic Specialists Conference.* 2009. Philadelphia, USA.
15. Gautero, L., et al. *Industrial approach for the deposition, through-vias wet opening and firing activation of a backside passivation layer applied on solar cells.* in *Proceedings of the 23rd European Photovoltaic Solar Energy Conference.* 2008. Valencia, Spain.
16. Specht, J., et al. *Using hotmelt-inkjet as a structuring method for higherefficiency industrial silicon solar cells.* in *Proceedings of the International Conference on Digital Printing Technologies and Digital Fabrication.* 2008. Pittsburgh, PA, USA.
17. Wolf, A., et al., *Comprehensive analytical model for locally contacted rear surface passivated solar cells.* Accepted for publication in Journal of Applied Physics, 2010.
18. Kania, D., et al. *High temperature stability of PECVD aluminium oxide layers applied as negatively charged passivation on c-Si surfaces.* in *This Conference, 25th EUPVSEC.* 2010. Valencia.
19. Fischer, B., *Loss analysis of crystalline silicon solar cells using photoconductance and quantum efficiency measurements,* in *Fachbereich Physik.* 2003, Universität Konstanz: Konstanz. p. 198.
20. Saint-Cast, P., et al. *P-type Cz-si perc solar cells applying PECVD aluminum oxide rear surface passivation.* in *This Conference, 25th EUPVSEC.* 2010. Valencia.